Available online at www.sciencedirect.com

ScienceDirect

ELSEVIER

Coordination Chemistry Reviews 252 (2008) 2528–2539

COORDINATION
CHEMISTRY REVIEWS

www.elsevier.com/locate/ccr

Review

Controlling electron exchange in molecular assemblies

Andrew C. Benniston, Anthony Harriman *

Molecular Photonics Laboratory, School of Natural Sciences, Bedson Building Newcastle University, Newcastle upon Tyne NE1 7RU, United Kingdom

Received 28 August 2007; accepted 3 October 2007
Available online 9 October 2007

Contents

Abstract

This review covers aspects of research conducted within the Molecular Photonics Laboratory at Newcastle University over the past 5 years. The research seeks to control the dynamics and direction of electron-exchange processes taking place in donor–spacer–acceptor molecular assemblies, where both donor and acceptor are transition metal poly(pyridine) complexes. Attention is focused on three key themes; namely, how the conformation of a biphenyl unit modulates the rate of triplet-energy transfer along the molecular axis, how to promote rapid triplet-energy transfer along the molecular axis, and how to direct electron exchange along a preferred pathway. The work is part of a larger project seeking to build artificial neural networks operating under light illumination.

Keywords: Photophysics; Triplet state; Metal complexes; Molecular electronics; Energy transfer

---

Abbreviations: FWHM, full-width at half-maximum for a charge-transfer absorption band; HOMO, highest occupied molecular orbital; ILET, interligand electron transfer; IVCT, intervalence charge transfer; k_{ET}, rate constant for electron transfer; k_{EX}, rate constant for electron exchange; LUMO, lowest unoccupied molecular orbital; MLCT, metal-to-ligand charge-transfer; N, total number of repeat units that combine to form the spacer; Os, osmium(II); R_{MM}, distance between the metal centres; Ru, ruthenium(II); S_0, ground state; S_1, first-excited singlet state; terpy, 2,2′:6′,2″-terpyridine; T_1, first-excited triplet state; V_{DA}, electronic coupling matrix element; $V_{DA}^{(i)}$, effective coupling element for the ith residue in the spacer; V_0, electronic coupling matrix element at orbital contact; α_{BA}, atomic orbital coefficient describing coupling between spacer and acceptor; α_{DB}, atomic orbital coefficient describing coupling between donor and spacer; β, attenutation coefficient for electronic coupling between donor and acceptor; bipy, 2,2′-bipyridine; d, separation distance; δ, coupling between the adjacent subunits comprising the spacer unit; δ_0, coupling between the adjacent subunits when held in a planar geometry; ε_{MAX}, molar absorption coefficient at the peak maximum; ΔE_{DB}, energy gap between orbitals of donor and spacer units; ΔG°, change in Gibbs free energy; $\Delta G^\#$, change in free energy of activation; ϕ, torsion angle between adjacent phenyl rings; FCWD, Franck-Condon weighted density of states; $h\omega$, intramolecular vibrational mode; $h\omega_M$, medium-frequency intramolecular vibrational mode; λ, total reorganisation energy; ν_{MAX}, absorption maximum for a charge-transfer transition in units of wave number.

* Corresponding author. Tel.: +44 191 222 8660; fax: +44 191 222 8660.
E-mail address: anthony.harriman@ncl.ac.uk (A. Harriman).

0010-8545/$ – see front matter © 2007 Elsevier B.V. All rights reserved.
doi:10.1016/j.ccr.2007.10.006

1. Introduction

It is generally accepted that a comprehensive understanding of electron-transfer processes is essential for further progress in many fields of chemistry, biology, physics and biochemistry [1]. The diversity of research dependent on electron-transfer processes spans from biological enzymes [2,3] to opto-driven devices [4], and requires an in-depth knowledge of how electrons and/or holes move through a wide variety of materials. This point is probably best exemplified by the hot debate that has taken place over recent years of the electron/hole transport properties of double-stranded DNA, and the concept that the base-pairs act as an efficient highway for charge migration [5,6]. Charge transport in biological systems can be viewed as occurring in complex 3D architectures, and detailed structural information is generally required to fully understand the process [7,8]. By comparison, molecular-based assemblies constructed to act as artificial mimics by which to probe electron-transfer events can be deemed as structurally less demanding [9]. It should not be viewed that such systems are easy to synthesise, and in fact this is not the case for many examples found in the literature [10,11]. These systems generally comprise electron donor and acceptor subunits connected via an organic spacer unit. This linking group has the dual role of providing a structural scaffold for the electrode-active terminals and acting as a conduit for the rapid and efficient transfer of electronic information along the molecular axis. There have been many different spacers proposed for use in concurrence with through-bond electron transfer or electron exchange [12,13]. The dynamics of information transfer along these molecular spacers (often termed as bridges or wires) is very much dependent on their chemical composition; for example, the hybridisation state of any connecting carbon units [14]. In directly fused aromatic units (e.g., phenyl, thiophene and pyrrole), electronic coupling along the poly(aryl)-based molecular wire would be expected to be modulated by the mutual orientation of adjacent aryl rings [15]. Rapid transfer is predicted for the case where all the rings are aligned in a coplanar geometry, but transfer will be seriously impaired if several rings are held in a mutually orthogonal orientation [16]. A superb example of this feat concerns the single-molecule conductance measurements made for a series of spacer groups suspended between metallic electrodes [17]. Here, the conductance shows a marked dependence on the central torsion angle and decreases as the aryl rings become increasing more orthogonal. The ability to manipulate the relative orientation of rings offers a fascinating means by which to control or gate the electron flux, which in principal could be used to direct information along predetermined pathways (Fig. 1a) [18]. Of course, there remains the serious problem of precisely how to switch conformations between the “on” and “off” positions in a reversible fashion.

An alternative strategy to manipulate the flow of information along a molecular axis spanning some 100 Å or so is to utilise the rather disparate chemistry that can be attained from different types of excited states or from similar states of very different energy. The basic concept here is to set up a competition between two possible chemical processes, for example, these might be intramolecular energy or electron transfer steps (Fig. 1b), but many other pairs of light-induced reactions are possible. The goal now is to direct the chemistry along one particular direction by careful balancing of the entire system, by perturbation of one small part of the spacer unit [19–21] or by changing the experimental conditions. Perhaps the most elegant way to achieve such possibilities is to use different input photon frequencies such that dissimilar excited states are populated by excitation. Provided these states have unique properties it should be possible to drive either electron transfer to an adjacent acceptor or energy transfer to a relay followed by further electron transfer. The advantage of this latter method is that no conformational switching is required, this being an essential feature of most other procedures considered for directing information flow in molecular assemblies, which would require some form of external input (i.e., electrons, protons and ions) [22,23]. However, the design element for molecular arrays such as that outlined in Fig. 1b is far more complex since all the individual components are required to play a precise role in promoting the requisite reactions. With this in mind, identification of the components for each specified task is paramount, and can be realised only by fundamental photophysical studies made on simpler molecular structures. This approach, of course, is very time consuming but benefits from the fact that the final array incorporates all the positive feedback from the preliminary work.

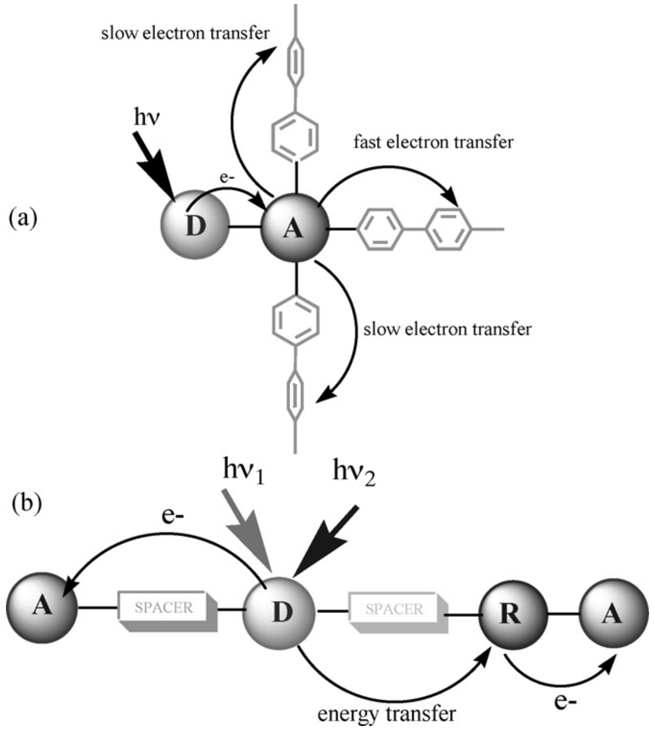

Fig. 1. (a) Concept of directing electron flow by controlling the torsion angle of a biphenyl unit. (b) Directional electron transfer using light of different frequency to instigate energy transfer to a relay (R).

Over the past few years, we have been actively engaged in the examination of artificial neural networks and have carried-out substantial studies along the themes outlined above [24]. Many of these studies have centred around photoactive ruthenium/osmium poly(pyridine) complexes [25,26] and on porphyrin-based arrays [27,28]. Mostly, we have used 2,2′:6′,2″-

terpyridine complexes because they are well suited to the construction of linear multi-component arrays but this simple strategy has introduced major problems in itself. Most notably, the triplet lifetimes and emission probabilities of Ru–terpy derivatives (terpy = 2,2′:6′,2″-terpyridine) are too low for the chromophore to be a useful reagent in our type of work and we have relied on functionalisation at the 4′-position with ethyne groups to overcome this particular problem [29]. In turn, this has necessitated a full investigation of the photophysical properties of ethyne-based Ru–terpy and Os–terpy complexes. Additional research has gone into identifying suitable spacer moieties that promote efficient intramolecular energy transfer [30]. We now summarise some of the more important milestones reached during this research programme and illustrate where the work is heading, with specific reference to the fabrication of molecular photonic devices.

2. Theoretical background

In order to properly manipulate selective charge migration in molecular systems, at least in a timely manner, it is essential that there exists a good understanding of the fundamental parameters governing such processes. It is recognised that Marcus theory [31] provides the starting point by which to relate the rate constant for intramolecular electron transfer (k_{ET}) with thermodynamic parameters. Thus, Eqs. (1)–(3) form the basis of the simplest level of underlying theory useful for designing molecular prototypes. Here, λ is the total reorganisation energy accompanying electron transfer and is the sum of contributions from both nuclear and solvent terms, V_{DA} is the electronic coupling matrix element and ΔG° is the change in Gibbs free energy during the electron-transfer step. The most significant aspect of Marcus theory is the change in free energy of activation $\Delta G^{\#}$ and its parabolic dependence on ΔG° and λ; evidently when $\Delta G^{\circ} = -\lambda$ electron transfer is activationless. It is also important to recognise that V_{DA} is predicted to decrease exponentially with increasing separation (d) between donor and acceptor units, according to Eq. (3). The attenuation factor β represents the conductivity of the bridging medium while V_0 is the coupling element at orbital contact:

$$k_{\mathrm{ET}} = \frac{2\pi}{\hbar} \frac{|V_{\mathrm{DA}}|^2}{\sqrt{4\pi k_{\mathrm{B}} T\lambda}} \exp\left(-\frac{\Delta G^{\#}}{k_{\mathrm{B}} T}\right) \tag{1}$$

$$\Delta G^{\#} = \frac{(\Delta G^{\circ} + \lambda)^2}{4\lambda} \tag{2}$$

$$V_{\mathrm{DA}} = V_0 \exp(-\beta d) \tag{3}$$

A great number of constraints exist with regard to the accurate application of Eqs. (1)–(3) and care must be taken when interpreting experimental results along these lines. Even so, Marcus theory is extremely useful for designing molecular systems from first principles and there have been many studies over the past few years to determine how k_{ET} depends on the chemical composition of the donor–acceptor dyad and especially on the role of the spacer unit [32]. The crucial factor is the coupling element and the rational design of advanced molecular dyads requires an improved knowledge of how to control V_{DA} at the molecular level [33].

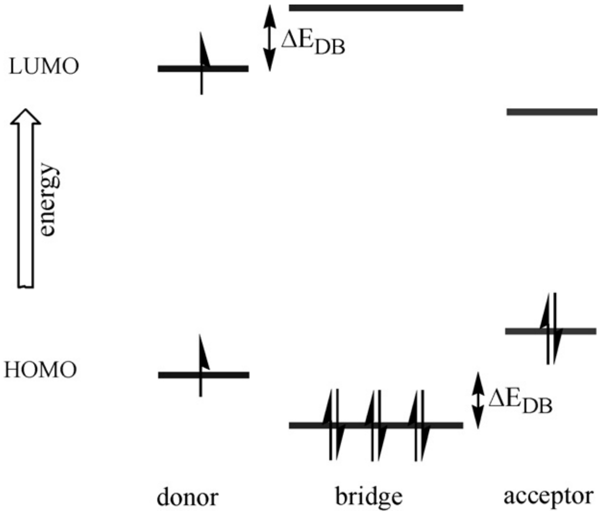

Fig. 2. Illustration showing the role of the bridge in promoting electron exchange using orbitals on the spacer unit.

2.1. Electronic coupling and super-exchange

Theory allows us to design multi-component molecules for particular purposes, subject to synthetic feasibility, and it is now possible to work out the required structure in quite fine detail. Regarding the construction of a molecular photonic device, however, it seems logical to insist that the electron transfer mechanism involves a through-bond process. Here, “virtual” orbitals localised on the bridge promote electron transfer from donor to acceptor, despite the fact that the spacer does not figure as a real intermediate in the electron-transfer process. Thus, electron transfer uses the spacer LUMO whilst hole transfer takes electrons from the HOMO of the spacer (Fig. 2). This type of reaction is commonly termed as the “super-exchange” mechanism [34,35] and has been used as the basis for understanding long-range electron transfer in molecular dyads. It should be stressed at this point that long-range electron transfer and electron exchange are treated as being equivalent in terms of super-exchange theory. The only real difference is that electron exchange involves simultaneous transfer of both an electron and a positive hole.

Super-exchange theory predicts that the coupling element is related to the energy gap (ΔE_{DB}) between relevant orbitals on the donor and on the spacer (Eq. (4)) [36]. Here, a slow rate of electron transfer is associated with a large energy gap and hence relatively weak electronic coupling. For a given donor, ΔE_{DB} is determined by the electronic properties of the spacer and some of the best materials seem to be poly(aromatics), diethynylated aromatics and diethenylated aromatics. The magnitude of V_{DA} also requires knowledge of the individual atomic orbital coefficients that describe coupling between the donor and first member of the spacer (α_{DB}), and between the last member of the spacer and the acceptor (α_{BA}). This extremely simple expression holds provided the energy gap ΔE_{DB} is much larger than the coupling energy between adjacent units in the spacer. In reality, this means that orbitals localised on the spacer must lie at much higher energy than those on the donor for the super-exchange mechanism to hold. More complicated expressions are available, indeed Eq. (4) is a unique solution to a general case [37], but these do not help in the design of molecular systems . . . their value lies in assisting the interpretation of kinetic data [38,39]:

$$V_{\mathrm{DA}} = \frac{\alpha_{\mathrm{DB}}\alpha_{\mathrm{BA}}}{\Delta E_{\mathrm{DB}}} \tag{4}$$

As discussed previously, according to Eq. (3) k_{ET} should decrease rather sharply with increasing separation of the reactants. However, several cases have been found [38,39] where the fall-off in rate is much less than predicted, and the attenuation coefficient β seems to vary with the length of the bridge or with solvent polarity [40]. These observations have been interpreted in terms of a change in the electron-transfer mechanism from long-range to sequential (or hopping) mechanisms [41]. In this latter case, long-range electron transfer is achieved by way of a cascade of short-range steps, each occurring by way of super-exchange. Both mechanisms can operate simultaneously, their relative importance depending on the experimental conditions:

$$\left\langle V_{\mathrm{DA}}^2 \right\rangle = \frac{1}{N}\sum_{i=1}^{N} (V_{\mathrm{DA}}^{(i)})^2 \tag{5}$$

That a bridge rarely functions as a single electronic entity [33,37] is an additional complication. Conventional metallic wires have a well-defined resistivity that increases in proportion to their length. By comparison, molecular conductors comprise a series of discrete orbitals that offer a disparate level of resistivity. This has the overall effect of affording a discontinuous conduit with regions of high and low conductivity. Thus, Eq. (5) offers a better description of the coupling element and now $V_{\mathrm{DA}}^{(i)}$ is an effective coupling element for the ith residue in the spacer, and N is the total number of repeat units that combine to form the spacer [37].

2.2. Nuclear tunnelling and quantum mechanical effects

The Marcus equation [31] predicts that once the driving force for electron transfer exceeds the reorganisation energy the rate of electron transfer should drop off quite dramatically. However, experimental studies have shown that the activation energies for electron-transfer processes occurring in the so-called Marcus inverted region ($\Delta G^{\circ} < -\lambda$) are often substantially less than those predicted on the basis of Eq. (2) [42]. This effect has been attributed to some of the excess thermal energy being transferred to intramolecular vibrational modes ($h\omega$) associated with the donor or acceptor. The net effect is to lower $\Delta G^{\#}$ by an amount corresponding to a certain number of quanta of energy $h\omega$. The semi-classical version of the theory developed by McConnell (Eqs. (6) and (7)) is based on the inclusion of a single, medium-frequency vibrational mode ($h\omega_{\mathrm{M}}$) [43]:

$$k_{\mathrm{ET}} = \frac{2\pi}{\hbar}\frac{V_{\mathrm{DA}}^2}{\sqrt{2\pi\sigma^2}} \exp\left(-\frac{(\Delta G^{\circ}+\lambda)^2}{2\sigma^2}\right) \tag{6}$$

$$\sigma^2 = \lambda h\omega_{\mathrm{M}} \coth\left(\frac{h\omega_{\mathrm{M}}}{2k_{\mathrm{B}}T}\right) \tag{7}$$

There is one further problem for understanding the rates of electron transfer that fall within the inverted region and that involves nuclear tunnelling; this phenomenon is especially important at low temperature [44]. This process has the effect of by-passing the normal transition state, since the electron can tunnel through a narrow barrier. Nuclear tunnelling has been observed for donor–acceptor pairs held in close proximity [45] and where one particular vibrational mode plays a key role. The main effect of nuclear tunnelling is that k_{ET} becomes independent of temperature. It has to be stressed, however, that the rate constant for electron transfer occurring via nuclear tunnelling is relatively low.

3. A variable resistor based on the geometry of the spacer unit

There has been some notable work carried out over the past decade or so to try and ascertain precisely how a change in the geometry of the spacer unit affects the dynamics of through-bond electron-transfer processes [34,35]. The particular aspect of the spacer geometry that concerns us here is a gross change in structure that might be used as the basis for an off-on switch and we have focused our attention on the torsion angle between adjacent phenylene rings. Theoretical calculations have indicated that the overall electronic resistivity of an electronic conduit depends on how well molecular orbitals on adjacent subunits overlap to form a continuous medium [33,27]. This is certainly true in the case of a 4,4′-biphenyl unit where the angle between the two phenyl rings will influence the extent of electron delocalisation. The first attempt to exploit this effect was made by McLendon et al. [46] who used 4,4′-biphenyl as a bridge between different porphyrin termini and varied the dihedral angle between the phenyl rings by substitution at the 2,2′-positions. It was observed that the rate of through-bond electron transfer was dependent on the angle around the central biphenyl linkage and reached a minimum at 45°. This finding is contradictory to theory [47], at least for an intramolecular system [48], and it is important to realise that changes in the nature of the substituents will also have significant effect on the electronic properties of the bridge. Despite this reservation, a clear correlation between the conductance through a single molecule suspended between macroscopic electrodes and the central torsion angle has been found for a series of substituted biphenyl-based analogues [17]. Here, the conductance increases as a $\cos^2$ function of the torsion angle, as predicted by theory:

3.1. Strapped biphenyl units as spacers

The approach we have taken is to tether a strap across the 2,2′-positions, thereby keeping a constant substitution pattern, and using the strap length to control the central torsion angle (Fig. 3) [49]. The electronic coupling element in these cases can be described in terms of Eq. (8) where δ refers to coupling between the adjacent phenyl rings (Eqs. (8) and (9)). From Eq.

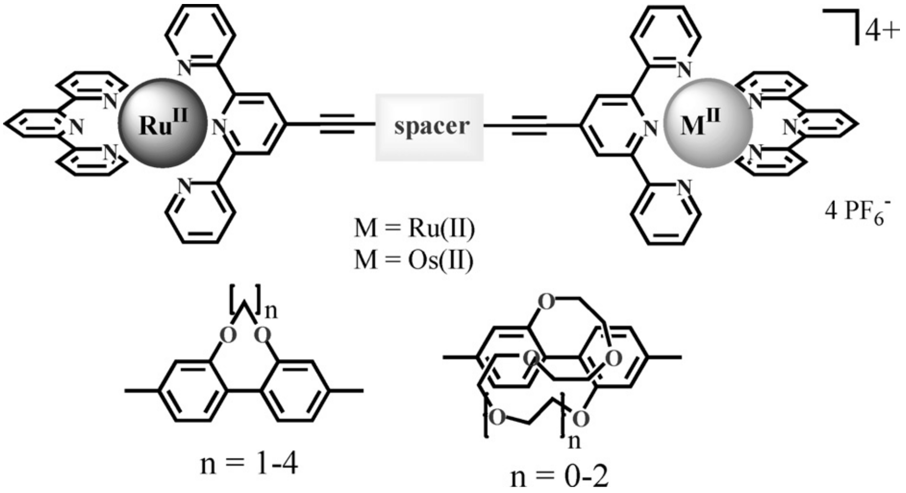

Fig. 3. Model systems used to measure the effect of torsion angle on electron exchange, where the length of the strap controls the size of the angle.

(9), the value of δ can be related to the torsion angle ϕ by reference to coupling at 0° (δ_0). By varying the length of the strap, a range of torsion angles can be obtained, but it should not be forgotten that thermal fluctuations have to be taken into account. This latter problem can be overcome, at least to a large extent, by embedding the sample in a low-temperature glassy matrix. The series of compounds containing the crown ether linkers facilitate coordination of cations inside the central void which serve to rigidify the crown and impose a restricted torsion angle around the central biphenyl group (Fig. 4) [50]. It is thus possible to sample a considerable variety of angles without serious perturbation of the electronic properties.

$$V_{\mathrm{DA}} = \frac{\alpha_{\mathrm{DB}}\alpha_{\mathrm{BA}}}{\delta}\left|\frac{-\delta}{\Delta E_{\mathrm{DB}}}\right|^2 \qquad (8)$$

$$\delta = \delta_0(\cos\phi)^2 \qquad (9)$$

3.2. Hole transfer in strapped biphenyl-based dyads

Having prepared the first systematic series of donor–spacer–acceptor dyads displaying a variable torsion angle but comparable, if not identical, electronic properties the next issue is to devise experiments to measure the extent of electronic coupling along the molecular axis. The first set of measurements was made with the corresponding series of strapped quaterphenyl derivatives where the dihedral angle was varied by the same strategy [51]. These compounds are strongly fluorescent and allow classical photophysical properties to be made in both solution and frozen glasses. We were able to establish that the optical properties, especially those of the first-excited singlet state, are related to the torsion angle set by the strap. Interestingly, the properties of the triplet-excited state were less dependent on strap length [51]. For the symmetrical Ru/Ru binuclear dyads, which are weakly luminescent at ambient temperature, photophysical studies are more demanding but it proved possible to examine the strength of electronic communication in these molecules by recording optical absorption spectra for the corresponding mixed-valence complexes formed by selective oxidation of one metallo-terminal; the new charge transfer transition seen in the near infrared region is due to charge hopping between the two terminals [52]. In these complexes, where $\Delta G^\circ = 0$, the size of V_{DA} can be calculated

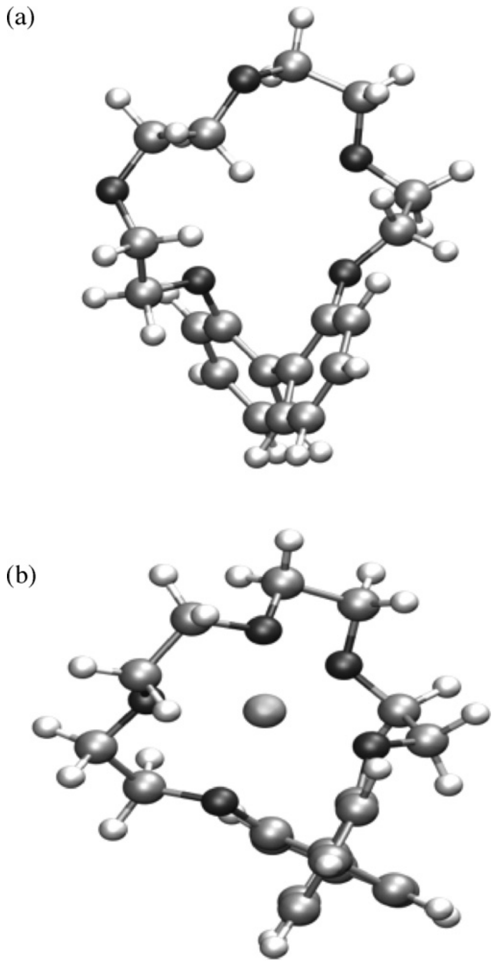

Fig. 4. Molecular model of a crown-5 ether bridge showing (a) the expanded polyether strap and (b) the resultant structure upon cation binding to three of the possible five oxygen atoms.

directly from Eq. (10) [53]. Here, $\varepsilon_{\mathrm{MAX}}$ is the molar absorption coefficient at the peak maximum, ν_{MAX} is the absorption maximum in cm^{-1} and FWHM is the full-width at half maximum of the Gaussian-shaped absorption band. The charge-transfer length R_{MM} is simply taken as the distance between the metal centres, although it is realised that this is a crude assumption:

$$V_{\mathrm{DA}} = \frac{0.0206}{R_{\mathrm{MM}}}\sqrt{\varepsilon_{\mathrm{MAX}}\nu_{\mathrm{MAX}}\mathrm{FWHM}} \tag{10}$$

Using the intervalence charge-transfer methodology introduced by Reimers and Hush [54], we were able to quantify how changes in the torsion angle affect the magnitude of V_{DA} in the series of mixed-valence Ru–terpy complexes of the type shown in Fig. 3 [55]. The coupling is greatest at 0° and there is a progressive decrease with increasing dihedral angle until reaching a clear minimum at 90°. It is worth noting that coupling does not vanish at 90°. This observation can be rationalised by the fact that biphenyl-based spacer unit is subject to thermal fluctuations about the mean angle and also to the fact that electronic coupling can take place through the connecting single bond. The electronic coupling element for the above examples relates to hole transfer, using the HOMO orbitals of the bridge. Unfortunately, it is not possible to obtain kinetic data for this system since there is no obvious spectroscopic signature by which to monitor the event. This is a major drawback as one would like to have some appreciation of how big a variation in the rates of electron transfer can be achieved by rapid switching of the central torsion angle [17]. Indeed, a critical point for the design of putative optical-switches based on this approach is to compare rates of electron transfer through π orbitals (i.e., planar geometries) with those through σ orbitals (i.e., orthogonal geometries).

3.3. Electron delocalisation in biphenyl-based dyads

The binuclear ruthenium(II) complexes (Fig. 3) are not all weak phosphorescence in deoxygenated solution at ambient temperature but the triplet lifetime is kept relatively short by thermal population of high-lying metal-centred states that are themselves strongly coupled to the ground state. These thermal decay routes become inaccessible at low temperature, however, and quite strong emission is seen in a glassy matrix [56]. This simplification means it is easy to obtain rate constants (k_{NR}) for non-radiative decay of the emitting metal-to-ligand, charge-transfer (MLCT) triplet state under these conditions. We were able to show that k_{NR} depends on torsion angle, with the maximum rate being found at ca. 40° [57]. This finding was rather unexpected but can be accounted for if changes occur in the degree of electron delocalisation at the triplet level. Consequently, illumination of the metal complex results in rapid ejection of an electron from the metal-localised d-orbital to the LUMO localised on the substituted terpyridine ligand. Previous findings support the notion that the triple bond facilitates extended π-conjugation [58]. Hence, it is reasonable to suppose that the promoted electron can sample a sizeable fraction of the bridging ligand, but the central biphenyl group presents a barrier to full electron delocalisation unless it is held in a planar arrangement.

This concept of the torsion angle being able to control the extent of electron delocalisation is difficult to prove on the basis of these binuclear complexes since so many other factors influence the emission properties. To pursue the effect further, a series of strapped viologens was synthesised in which the length of the tether was again used to alter the central dihedral angle between the two pyridinium rings [59]. In this way, it becomes possible to monitor the effect of dihedral angle on the reduction potential, optical absorption properties of the parent viologen, intermediary π-radical cation and neutral viologen, and on the EPR properties of the π-radical cation. A comprehensive picture now emerges of the way in which the planarity of the bipyridinium unit affects the electronic properties of the molecule and, in particular, communication between the two rings. It is especially interesting to note the effect of torsion angle on the distribution of spin density at the π-radical cation stage.

$$k_{\mathrm{EX}} = \frac{2\pi}{\hbar}|V_{\mathrm{DA}}|^2\mathrm{FCWD} \tag{11}$$

3.4. Electron exchange in biphenyl-based mixed-metal complexes

The incorporation of an Os–terpy in place of one of the Ru–terpy terminals in the binuclear array facilitates intramolecular triplet-energy transfer across the biphenyl spacer. The primary mechanism for such a process involves Dexter-type electron exchange. This through-bond interaction involves simultaneous transfer of an electron (through the bridging LUMO) and a positive hole (through the bridging HOMO). The rate constant for electron exchange (k_{EX}) is given by Eq. (11), where the Franck-Condon weighted density of states (FCWD) can be calculated precisely from emission spectra recorded for isolated donor and acceptor species [60]. Thus, the coupling element can be derived directly from experimental data.

Using the above approach, we have explored the effect of dihedral angle on the rate of triplet-energy transfer in the series of mixed-metal complexes pertinent to Fig. 3. The rates of energy transfer are fairly fast, even at 77 K where the molecular geometry is locked into the lowest energy conformation. The results confirm that the maximum coupling occurs when the biphenyl group is coplanar (Fig. 5) [61]. There is a substantial decrease in V_{DA} as the torsion angle increases and a definite minimum at around 90°. As noted for the IVCT studies, the coupling element does not decrease to zero at an orthogonal geometry. Unlike in the hole transfer case, however, this is attributed to nuclear tunnelling across the connecting bond. It is interesting to note that the variation in k_{EX} reaches 80-fold as the angle increases from 0° to 90°. This is considered to be a sufficiently large variation to propose constructing a switch for directed electron exchange on the principle of rapid conformational exchange. This raises the question of how to bring about such a large scale conformational change and, in attempting to address this point, our attention has turned to the corresponding dibenzo[1,2]dithiine unit [62]. Here, electrochemical cleavage of the S–S bond gives rise to a major structural change from the near coplanar arrange-

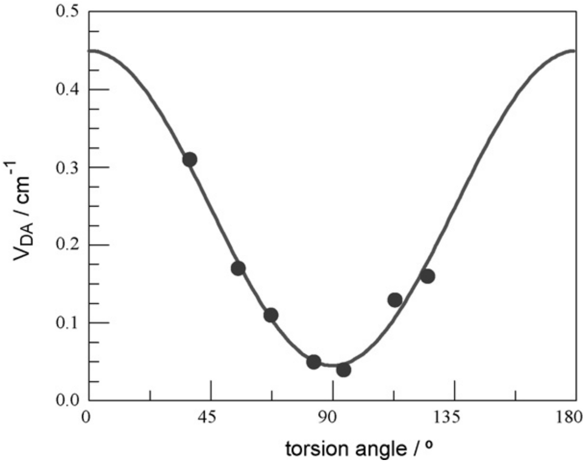

Fig. 5. Variation in the electronic coupling matrix element with changes in the torsion angle for the Ru/Os mixed-metal complexes.

ment to an orthogonal conformation (Fig. 6). This system is now under active investigation.

4. Getting the right relay

According to the simplified picture given as Fig. 2 the energies of the HOMO/LUMO orbitals resident on the spacer unit are critical in promoting Dexter-type energy transfer from donor to acceptor. Two limiting scenarios can be readily identified and applied to the specific case of triplet-energy transfer from Ru–terpy to Os–terpy along a linear spacer: If the triplet energy of the spacer greatly exceeds that of the donor, super-exchange is likely to be inefficient and energy transfer will not compete with deactivation of the excited state. This situation does not preclude energy transfer taking place because the Förster dipole–dipole mechanism might still operate but the factors controlling the rate will now be markedly different. Secondly, if the triplet energy of the spacer is too low this species becomes the final resting place for the absorbed photonic energy. This latter point is of special importance in cases where multiple organic units are linked together to create a wire-like structure [37], since conjugation should afford a diminished HOMO-LUMO gap. This situation is often observed for the S_0–S_1 band gap and it assumed that the same occurs for the corresponding T_1–S_0 band gap, although less direct spectroscopic information is available to support this latter hypothesis. The net result of this dichotomy is that it is still not possible to identify the optimum spacer unit for long-range energy transfer between this particular pair of reactants.

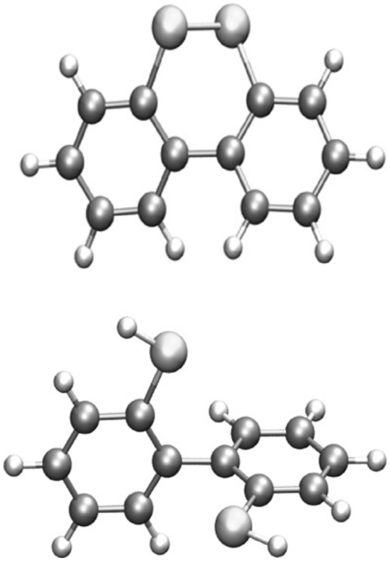

Fig. 6. Molecular models for dibenzo[1,2]dithiine in the closed (top) and open (bottom) forms.

4.1. Ethynylnaphthalene-based molecular rods

Taking account of a large volume of research from many laboratories concerned with fast triplet-energy transfer in Ru/Os poly(pyridine) complexes, it can be concluded that the ethynylnaphthalene unit [63,64] is the most promising module with which to construct superhighways for long-distance electron exchange. Why is this? The energy of the ethynylnaphthalene unit, being very close to that of the Ru-based donor and above that of the Os-based acceptor, is ideal for promoting Dexter-type electron exchange. According to the actual donor used, the ethynylnaphthalene triplet lies just above or slightly below the donor triplet [63,64] but even in the former case it can be accessed by thermal population at ambient temperature. As such, the spacer becomes an active, rather than passive, intermediate in relaying triplet energy along the molecular axis. The important point now is to examine how the triplet energy of the ethynylnaphthalene moiety evolves with increasing number of repeat units and this was done using a series of molecular rods, **NAP(n)** (Fig. 7).

In line with other studies made with oligomers based on, for example, thiophene, fluorene, and phenylene, there occurs a gradual shift to longer wavelength in the absorption maxima (from 428 nm for **NAP2** to 457 nm for **NAP6**)) with increasing number of naphthalene units [65]. Fluorescence is relatively intense for these molecular systems in fluid solution, and the emission spectral profiles display clear vibrational structure but poor mirror symmetry with the corresponding absorption bands. In view of the relatively large Stokes' shifts, it is concluded that the molecular rods become more planar upon promotion to the first-excited singlet state. A further shift towards planarity occurs on embedding the rods in a glassy matrix at 77 K. In contrast, the molecular rods are weakly phosphorescent in the frozen glass, but their triplet energies remain relatively constant across the series at around 1.88 eV. It also appears that, at the T_1 level, electronic coupling between adjacent naphthalene units is rather weak. Interestingly, the higher-lying triplet states, seen in laser flash photolysis studies, also exhibit features that are dependent of the number of repeat naphthalene units. Whereas the T_n triplet levels vary in energy across the series, the upper lying T_{n+1} levels are relatively insensitive to the oligomer length (Fig. 8).

4.2. Ethynylnaphthalene-based spacers

Having established the basic properties of the naphthalene-based oligomers, the next stage of development has involved

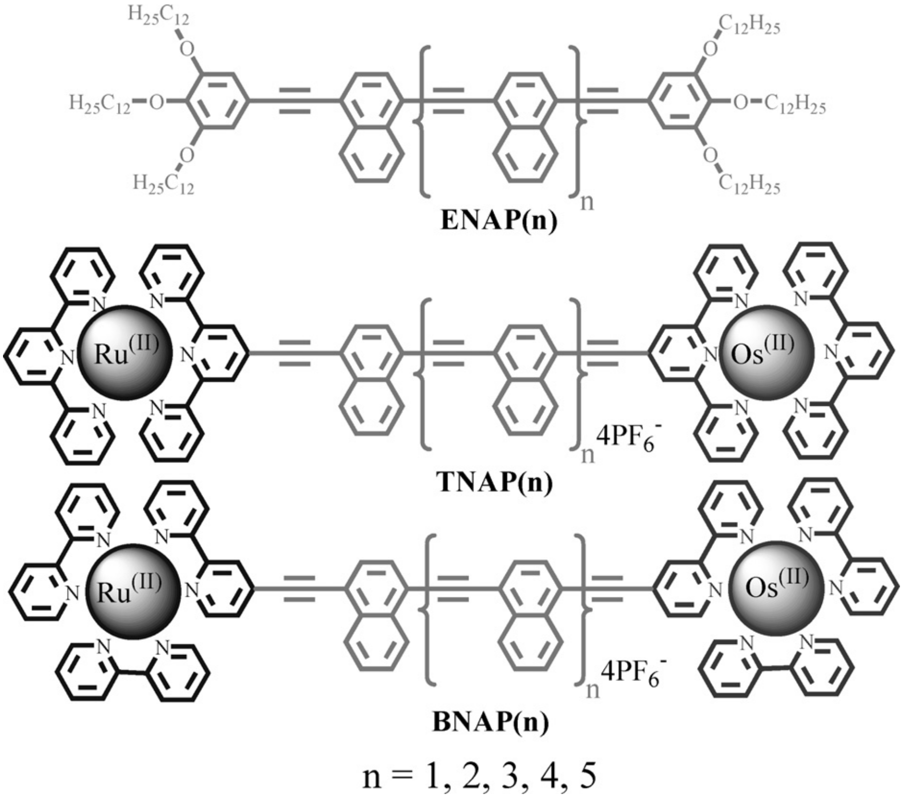

Fig. 7. Examples of hetero-bimetallic complexes incorporating naphthalene-based molecular bridges.

incorporation of the photoactive centres based on Ru–terpy and Os–terpy (Fig. 7). Using a multistep 'synthesis at metal' approach, a series of heteronuclear analogues has been produced for both terpy and bipy (bipy = 2,2′-bipyridine) series in order to elucidate the efficiency and rate of triplet-energy transfer along the molecular axis [66]. It is known that the basic photophysical properties of the Ru-based donor are strongly temperature dependent [56]. This can be attributed to coupling to high-lying *d–d* states that contribute to excited state deactivation. Furthermore, although phosphorescence takes place from the lowest energy metal-to-ligand, charge-transfer (MLCT) triplet state, there are upper-lying MLCT states that play a role in the overall photophysical processes. To avoid such complications, our initial studies focused on probing energy transfer in a low temperature glass [67]. A further advantage of the glassy matrix is that nuclear motions are at a minimum.

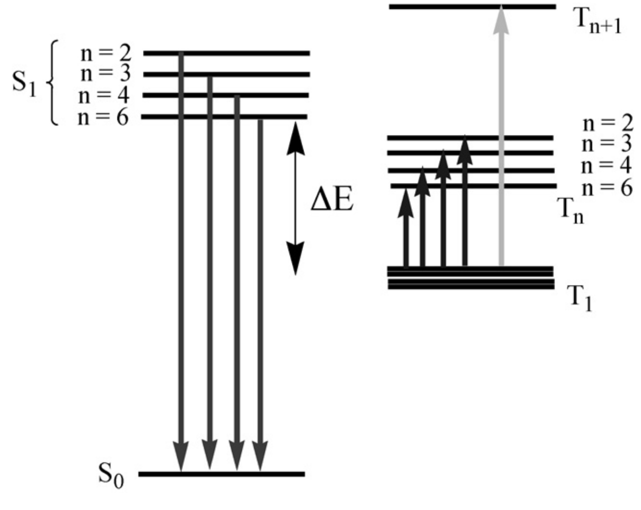

Fig. 8. Illustration showing how the first-excited singlet (S_1) and the various triplet states (T_1, T_n, T_{n+1}) vary with the number of naphthalene repeat units for **ENAP**(n).

In a frozen butyronitrile glass at 77 K, triplet-energy transfer within the series **TNAP**(n) was found to be >95% efficient, and despite the increase in molecular length, the rates varied only by a factor of five. An incoherent hopping mechanism was proposed to explain energy migration. Such a process firstly involves injection from the MLCT triplet state located on the Ru–terpy unit into the adjacent naphthalene unit. The thermodynamics are such that this process is reversible but further energy migration between subsequent naphthalene units leads to energy migration along the bridge. The overall process can be viewed as a one-dimensional random walk. The terminal Os–terpy unit is the final termination point for the photonic energy since its MLCT triplet state is much lower in energy than that of the spacer (Fig. 9). That is, at low temperature the energy gap is sufficiently large to inhibit thermal repopulation of the spacer triplet from the Os–terpy triplet. The results collected with the longer analogues are unambiguous in as much as there is a time lag between decay of the Ru–terpy triplet and formation of the corresponding Os–terpy triplet. Although the kinetics for these processes are not strictly first-order, it is clear that the donor triplet decays well before appearance of the acceptor triplet. This situation can only be explained in terms of a transient population of the naphtha-

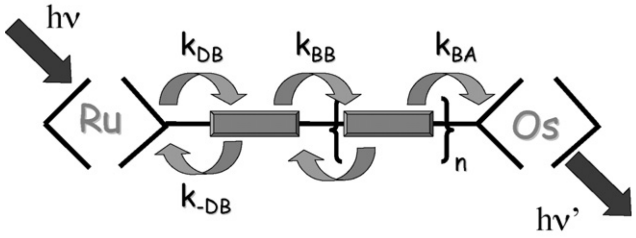

Fig. 9. Proposed incoherent energy-transfer hopping mechanism for the hetero-bimetallic complexes.

lene triplets located on the spacer; these being non-luminescent under the conditions used. Treating the kinetic data in terms of the simplified model shown as Fig. 9 allows estimation of the rate constant for photon hopping between adjacent naphthalene units. Incidentally, the efficiency of energy transfer along the molecular rod approaches 100% in all cases. For shorter bridges, there are indications that long-range super-exchange competes with short-range photon hopping.

Spectroscopic measurements have been completed for the corresponding solution-phase studies, where the rates are much faster [67]. Preliminary results are encouraging, and confirm that rapid and quantitative energy transfer takes place over a distance approaching 60 Å. Additional compounds have been synthesised for the bipy-based series that allow insertion of extra groups into the spacer function. This provides for improved understanding of the mechanism. It has to be stressed that a key feature of these systems relates to the unexpectedly weak electronic coupling between adjacent ethynylnaphthalene units. This is surprising in view of the connecting ethyne groups being expected to promote extensive electron delocalisation. The latter situation is seen for the S_1 states but not for T_1.

5. Directed processes

There have been many successful attempts to incorporate metal poly(pyridine) complexes into functional arrays that exploit their useful photophysical properties. For example, building Ru-bipy into a catanane equipped with two identical arms and a threaded crown ether provides the first realistic model of the redox asymmetry inherent to the bacterial photosynthetic reaction center [68]. Mostly, the metal complex has been used as chromophore and/or electron donor and few attempts have been made to use such complexes as electron or energy relays. Notable exceptions to this generalisation include porphyrin–metal complex dyads where both units can operate as chromophores [69–74,27]. In order to extend this field, it is necessary to generate asymmetric complexes where one of the coordinated ligands acts as energy or electron sink. Clearly, there is an advantage to focus on Ru–terpy, because the tridentate ligand facilitates construction of linear structures, and considerable research has gone into the synthesis of mono-functionalised Ru–terpy complexes. The most useful species are those bearing an acetylenic function at one of the 4′-positions. Thus, a single ethyne substituent lowers the reduction potential for that terpy ligand by ca. 200 meV and thereby introduces the required redox asymmetry. This has the effect of lowering the triplet energy, thereby pushing the emission wavelength into the near-IR, decreasing coupling with upper-lying metal centred states and prolonging the triplet lifetime by many orders of magnitude [75–78,25]. An additional effect is to enhance luminescence from an upper MLCT triplet state – the so-called fourth MLCT triplet – which lies ca. 1000 cm^{-1} above the lowest energy triplet [79]. The overall effect is to greatly increase the utility of the chromophore as a luminescent label or sensitiser. Similar effects have been noted for the corresponding Os–terpy complex [80].

5.1. Energy transfer in porphyrin–metal poly(pyridine) dyads

We can now consider how to further exploit the redox asymmetry introduced into the complex via insertion of a single 4′-ethyne substituent. Firstly, we note that the ethyne group can be reduced electrochemically, leading to the formation of polymers deposited on the electrode [81]. Perhaps more useful in the context of building photoactive arrays is the realisation that the triplet state associated with the substituted ligand lies at lower energy than that of the parent ligand. Charge injection under illumination, therefore, selectively produces the MLCT state with the promoted electron localised on the substituted ligand. This is important in that the system can be primed for electron or energy transfer along the molecular axis simply by adding relays to the open end of the ethyne group. In turn, this raises the question of how fast is interligand electron transfer (ILET) in metal terpy complexes.

After much debate [82], it is now well established that the MLCT triplet state has the electron density localised on a single poly(pyridine) ligand at any given moment. The promoted electron hops between the coordinated ligands in an incoherent manner. Experimental measurement of the rate of ILET is rendered difficult by the absence of obvious spectroscopic signatures and the most convincing evidence has accrued from time-resolved anisotropy studies. Here, the dynamics of ILET occur with characteristic time constants of 47 ps [83,84] and 8.7 ps [85], respectively, for Ru(II) and Os(II) tris(2,2′-bipyridine) complexes, where there is no thermodynamic driving force. In asymmetric complexes, the time scale for ILET increases and is notably faster for Os(II) than for Ru(II). A different approach for measuring the rate of ILET was introduced recently by Schoonover et al. [86] whereby this process was in competition with triplet-energy transfer to an appended anthracene residue. Related work by Hammarström and co-workers [87] found that electron transfer from the excited state of a Ru(II) tris(2,2′-bipyridine) complex to a covalently attached methyl viologen residue occurred within 4 ps and this rate seems to be at odds with the idea of fairly slow ILET. Subsequent studies [88] using ultra-fast laser excitation and transient absorption anisotropy measurements indicated that the ILET process is complete within 1 ps. Thus, there is a large variation in the reported rates of ILET in these complexes.

A problem with all experimental measurements reported to date, however, is that excitation produces a statistical mixture of MLCT triplet states wherein the promoted electron resides on

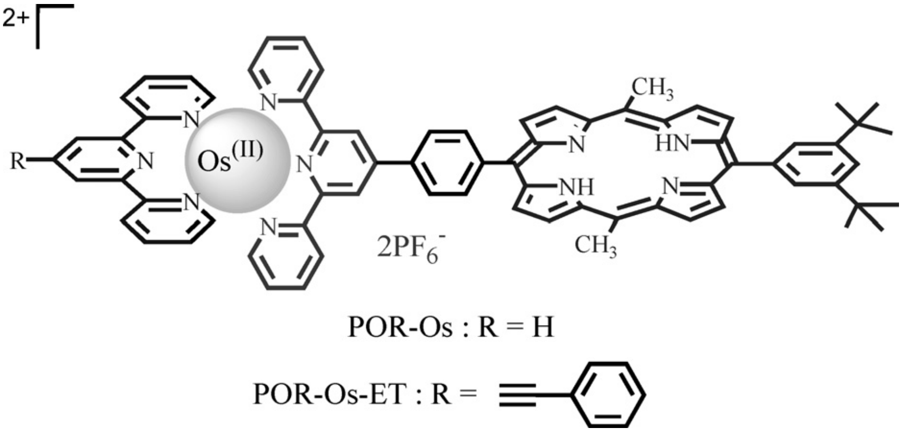

Fig. 10. Model systems used to study interligand electron transfer.

different ligands [86]. The experiment then involves monitoring the approach to equilibrium. We have sought to eliminate this difficulty using pulsed excitation of a porphyrin that is covalently attached to an Os(II)–terpy complex by way of a short spacer (Fig. 10) [89]. The singlet excited state of the porphyrin (S_1) so produced transfers excitation energy to the metal complex on a very fast time scale so as to generate the corresponding MLCT triplet state within a few picoseconds. The promoted electron resides solely on the proximal terpy ligand. Because the porphyrin possesses a low-lying triplet excited state (T_1), intramolecular triplet-energy transfer competes with ILET but energy transfer from the distal terpy ligand is relatively slow. This disparity in rates allows accurate screening of the ILET process [89].

For the parent system, POR–Os, evidence for ILET is derived solely from the statistical quality of fitting the kinetic data and there is no direct spectroscopic evidence to show that the distal terpy ligand is populated during the sequence of energy-transfer steps. The overall reaction scheme is shown below (Fig. 11) and the derived rate constants are collected in Table 1. According to this analysis, ILET accounts for about 30% of the initially formed proximal MLCT triplet state, the bulk undergoing triplet-energy transfer to populate the T_1 state localised on the porphyrin [89]. The thermodynamic position is that the proximal MLCT triplet is slightly lower in energy than the distal MLCT triplet and this accounts for the relatively slow rate of ILET in this system.

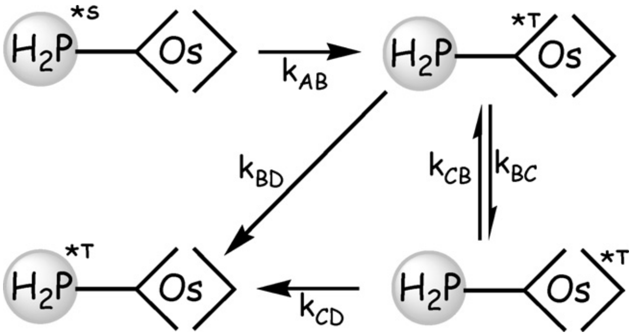

Fig. 11. Overall reaction process showing rapid formation of the proximal MLCT triplet state, followed by competition between triplet-energy transfer to the porphyrin $^3\pi,\pi$ state and ILET, as proposed for the porphyrin/Os–terpy dyads.

Turning attention now to POR–Os–ET (Fig. 10) it is notable that there is a small thermodynamic driving force for ILET from proximal to distal MLCT triplet states because of the effect of the ethyne substituent. The transient spectroscopic records again indicate that decay of the porphyrin S_1 state is extremely fast [89]. As for dyad POR–Os, it is assumed that energy transfer selectively populates the proximal MLCT triplet state localised on the metal complex. Formation of the porphyrin T_1 state is remarkably slow compared to POR–Os. Furthermore, global analysis indicates that formation of the porphyrin-based triplet state lags far behind decay of the S_1 state and does not correspond to a single exponential process. A complete analysis was made in accordance to Fig. 11 and the rate constants derived from a global analysis are collected in Table 1. In this case [89], the spectral records provide clear evidence for intermediate population of the MLCT triplet state but without specifying which terpy ligand is involved. The delayed formation of the T_1 state, however, can be explained only in terms of competing ILET since the thermodynamics and geometry for triplet-energy transfer from the proximal MLCT triplet to T_1 remain exactly the same as for POR–Os. Global analysis of the kinetic data shows that energy transfer from the proximal MLCT triplet state T_1 (k_{BD}) occurs at a rate comparable to that found for POR–Os under the same conditions but this step competes poorly with ILET to form the distal MLCT triplet state. The rate constant (k_{BC}) for this latter step is increased relative to POR–Os by a factor of approximately sixfold, presumably due to the improved thermodynamics. The

Table 1
Summary of the kinetic data derived by global fitting of the spectroscopic data obtained for the porphyrin/Os–terpy dyads in deoxygenated acetonitrile at room temperature

Rate constant (ps^{-1})	POR–Os	POR–Os–ET
k_{AB}	0.24	0.29
k_{BD}	0.063	0.060
k_{BC}	0.031	0.100
k_{CB}	0.100	0.023
k_{CD}	NA	0.018

rate constant (k_{CB}) for reverse population of the proximal MLCT triplet state is set by the equilibrium constant and is relatively small. The rate constant (k_{CD}) for triplet-energy transfer from the distal MLCT triplet state is low, compared to triplet-energy transfer from the proximal MLCT triplet state, because of the increased separation distance.

6. Conclusions

Progress has been made along three main directions. Indeed, we now have a complete description of how a change in the torsion angle between adjacent aryl rings affects the extent of electronic communication along the molecular axis. This has been done by a series of systematic studies, each involving a set of strapped biaryl spacers, and includes electron delocalisation, hole transfer, and electron exchange. The disparity in electronic coupling between orthogonal and planar geometries is sufficient to propose such structural changes as the basis for a molecular-scale switch and initial investigations to develop such an idea are underway. It might be noted that tethered biphenyls of this type are inherently chiral and this opens the possibility to explore the efficacy of electronic coupling along chiral bridges. There is no obvious reason to suppose that the electron transfer can discriminate in favour of left- or right-handed bridges but there might be an important chiral discrimination between charge separation and subsequent charge recombination. This possibility would lead to new ways to stabilise charge-separated states.

In quite separate research, we have identified ethynylnaphthalene units as being ideal building blocks for construction of molecular arrays capable of very long-range electron exchange. It should be stressed that this conclusion relates only to the use of Ru–terpy and Os–terpy terminals and arises because of the precise positioning of the relevant triplet-energy levels. Electron exchange is quantitative over more than 60 Å – the limit being set by solubility – and could be extended over much longer distances if required. The key point here has been the facile energy migration between adjacent ethynylnaphthalene units, which themselves remain in weak electronic communication. Each unit acts independently so that energy transfer resembles a one-dimensional random walk along the backbone. This feature is of extreme importance and prevents formation of a highly delocalised π-system where the triplet energy would fall below that of the acceptor. We are now in the process of increasing the dimensionality of these arrays by introducing junctions into what can be described as molecular-scale wires. The junctions help with solubility. An additional spin-off from these particular systems involves the observation that the ethyne substituent raises the profile of the so-called fourth MLCT triplet state localised on the metal terpy terminals. This state lies less than 1000 cm^{-1} above the lowest energy ensemble and can be accessed at ambient temperature. It is possible that, in certain circumstances, the fourth MLCT state could play an active role in long-range electron exchange.

The properties recorded for these ethynylnaphthalene spacers could make them valuable as a means by which to channel photons along molecular-scale light guides. Such materials are needed if molecular photonics is to challenge molecular electronics, and in particular the use of single-molecule electrochemistry. Thus, major advances have been made in our ability to suspend molecules between metallic electrodes and to measure their electrochemical response, notably their ability to conduct charge. The electrodes can be formed by a remarkably easy process and the sensitivity of the measurement technique has advanced to match the needs of the experimentalist. It has long been possible to monitor single-molecule fluorescence but we have no easy way to focus light down to the single-molecule level in an organised way. There are existing approaches to this problem using porous networks, usually zeolitic materials with well defined one-dimensional channels that can be stoppered with suitable molecules, but there still remains the problem of how to selectively isolate one particular channel. This issue needs to be resolved if we are to take advantage of the many important benefits offered by photochemistry. Our plan is to be build new types of light guide from ethynylnaphthalene units encapsulated within an insulating coating.

The final investigation described herein refers to ILET and, in particular, to the use of a porphyrin-type sensitiser to selectively excite one of two terpy ligands. We have successfully used this approach to measure the rates of ILET for certain Os–terpy complexes but the situation is far from clear. That ILET is fast remains undoubted but there is a wide dispersity in the rates measured by different approaches and for different systems. Fortunately, the rate of ILET is sufficiently fast for our purposes and it is clear that multi-component molecular systems can be built that incorporate Ru–terpy or Os–terpy units as active relays. We have in mind to construct intricate arrays based on these materials that allow the direction of electron transfer to be controlled by changing the frequency of the incident laser beam.

Acknowledgements

We thank the EPSRC (GR/S00088/01, EP/C007727/1 and EP/D032946/1) and Newcastle University for financial support. The efforts of a large number of talented postgraduate and postdoctoral associates are recognised and we thank all our co-workers for their invaluable input into this research.

References

[1] V. May, O. Kühn, Charge and Energy Transfer Dynamics in Molecular Systems, Wiley-VCH, Berlin, 2001.
[2] S. Calabrese Barton, J. Gallaway, P. Atanassov, Chem. Rev. 104 (2004) 4867.
[3] M.W. Makinen, S.A. Schichman, S.C. Hill, H.B. Gray, Science 222 (1983) 929.
[4] J.L. Brédas, J.P. Calbert, D.A. da Silva Filho, J. Cornil, Proc. Natl. Acad. Sci. U.S.A. 99 (2002) 5804.
[5] U. Diederichsen, Angew. Chem., Int. Ed. Engl. 36 (1997) 2317.
[6] A. Harriman, Angew. Chem., Int. Ed. 38 (1999) 945.
[7] J. Diesenhofer, E. Opp, R. Miki, R. Huber, H. Michel, Nature 318 (1985) 618.
[8] K.N. Ferreira, T.M. Iverson, K. Maghlaoui, J. Barber, S. Iwata, Science 303 (2004) 1831.
[9] M.R. Wasielewski, Chem. Rev. 93 (1992) 435.
[10] Y. Nakamura, N. Aratani, A. Osuka, Chem. Soc. Rev. 36 (2007) 831.
[11] S. Saha, J.F. Stoddart, Chem. Soc. Rev. 36 (2007) 77.
[12] E. Galoppini, Coord. Chem. Rev. 248 (2004) 1283.

[13] M.N. Paddon Row, Acc. Chem. Res. 27 (1994) 18.

[14] A.C. Benniston, A. Harriman, V. Grosshenny, R. Ziessel, New J. Chem. 21 (1997) 405.

[15] S. Woitellier, J.P. Launay, C. Joachim, Chem. Phys. 131 (1989) 481.

[16] C. Liang, M.D. Newton, J. Phys. Chem. 96 (1992) 2855.

[17] L. Venkataraman, J.E. Klare, C. Nuckolls, M.S. Hybertsen, M.L. Steigerwald, Nature 442 (2006) 904.

[18] A.C. Benniston, Chem. Soc. Rev. 33 (2004) 573.

[19] M. Hissler, A. Harriman, P. Jost, G. Wipff, R. Ziessel, Angew. Chem., Int. Ed. 37 (1998) 3249.

[20] M. Hissler, A. El-ghayoury, A. Harriman, R. Ziessel, Angew. Chem., Int. Ed. 37 (1998) 1717.

[21] A. Harriman, A. Mayeux, C. Stroh, R. Ziessel, Dalton Trans. (2005) 2925.

[22] A.R. Pease, J.O. Jeppesen, J.F. Stoddart, Y. Luo, C.P. Collier, J.R. Heath, Acc. Chem. Res. 34 (2001) 433.

[23] V. Amendola, L. Fabbrizzi, M. Liccelli, C. Mangano, P. Pallavinci, L. Parodi, A. Poggi, Coord. Chem. Rev. 192 (1999) 649.

[24] A.C. Benniston, A. Harriman, Chem. Soc. Rev. 35 (2006) 169.

[25] A.C. Benniston, V. Grosshenny, A. Harriman, R. Ziessel, Dalton Trans. (2004) 1227.

[26] A.C. Benniston, A. Harriman, F. Romero, R. Ziessel, Dalton Trans. (2004) 1233.

[27] A.C. Benniston, A. Harriman, C. Pariani, C.A. Sams, Phys. Chem. Chem. Phys. 8 (2006) 2051.

[28] A.C. Benniston, G.M. Chapman, A. Harriman, M. Meyrabi, J. Phys. Chem. A 108 (2004) 9026.

[29] A.C. Benniston, A. Harriman, V. Grosshenny, R. Ziessel, Angew. Chem., Int. Ed. Engl. 33 (1994) 1884.

[30] A.C. Benniston, S. Mitchell, S.A. Rostron, S. Yang, Tetrahedron Lett. 45 (2004) 7883.

[31] R.A. Marcus, N. Sutin, Biochim. Biophys. Acta 811 (1985) 265.

[32] J.R. Reimers, N.S. Hush, J. Phys. Chem. A 103 (1999) 3066.

[33] J.R. Reimers, N.S. Hush, Nanotechnology 7 (1996) 417.

[34] C.A. Naleway, L.A. Curtiss, J.R. Miller, J. Phys. Chem. 95 (1991) 8434.

[35] K. Kilså, J. Kajanus, J. Mårtensson, B. Albinsson, J. Phys. Chem. B. 103 (1999) 7329.

[36] N.P. Redmore, I.V. Rubtsov, M.J. Therein, J. Am. Chem. Soc. 125 (2003) 8769.

[37] N.S. Hush, Ann. NY Acad. Sci. 1006 (2003) 1.

[38] M.P. Eng, B. Albinsson, Angew. Chem., Int. Ed. 45 (2006) 5626.

[39] M.P. Eng, T. Ljungdahl, J. Mårtensson, B. Albinsson, J. Phys. Chem. B 110 (2006) 6483.

[40] W.B. Davis, M.A. Ratner, M.R. Wasielewski, J. Am. Chem. Soc. 123 (2001) 7877.

[41] R.H. Goldsmith, L.E. Sinks, R.F. Kelley, L.J. Betzen, W. Lui, E.A. Weiss, M.A. Ratner, M.R. Wasielewski, Proc. Natl. Acad. Sci. U.S.A. 102 (2005) 3540.

[42] G. Pourtois, D. Beljonne, J. Cornil, M.A. Ratner, J.L. Brédas, J. Am. Chem. Soc. 124 (2002) 4436.

[43] H.M. McConnell, J. Chem. Phys. 35 (1961) 508.

[44] M. Bixon, J. Jortner, Faraday Discuss. Chem. Soc. 74 (1982) 17.

[45] A. Harriman, J.P. Rostron, M. Cesario, G. Ullrich, R. Ziessel, J. Phys. Chem. A 110 (2006) 7994.

[46] A. Helms, D. Heiler, G. McLendon, J. Am. Chem. Soc. 113 (1991) 4325.

[47] I.V. Rubtsov, N.P. Redmore, R.M. Hochstrasser, M.J. Therien, J. Am. Chem. Soc. 126 (2004) 2684.

[48] R.J. Cave, P. Siders, R.A. Marcus, J. Phys. Chem. 90 (1986) 1436.

[49] A.C. Benniston, A. Harriman, P.Y. Li, C.A. Sams, Tetrahedron Lett. 44 (2003) 4167.

[50] A.C. Benniston, P.Y. Li, C.A. Sams, Tetrahedron Lett. 44 (2003) 3947.

[51] B.D. Allen, A.C. Benniston, A. Harriman, I. Llarena, C.A. Sams, J. Phys. Chem. A 111 (2007) 2641.

[52] J.P. Launay, Chem. Soc. Rev. 30 (2001) 386.

[53] N.S. Hush, Trans. Faraday Soc. 91 (1961) 557.

[54] J.R. Reimers, N.S. Hush, Inorg. Chem. 29 (1990) 3686.

[55] A.C. Benniston, A. Harriman, P.Y. Li, C.A. Sams, M.D. Ward, J. Am. Chem. Soc. 126 (2004) 13630.

[56] A. Amini, A. Harriman, A. Mayeux, Phys. Chem. Chem. Phys. 6 (2004) 1157.

[57] A.C. Benniston, A. Harriman, P.Y. Li, P.V. Patel, C.A. Sams, Phys. Chem. Chem. Phys. 7 (2005) 3677.

[58] A.C. Benniston, G.M. Chapman, A. Harriman, M. Mehrabi, C.A. Sams, Inorg. Chem. 43 (2004) 4227.

[59] A.C. Benniston, A. Harriman, P.Y. Li, J.P. Rostron, W. Clegg, R.W. Harrington, Chem. Eur. J., in press.

[60] Z. Murtaza, D.K. Graff, A.P. Zipp, L.A. Worl, W.E. Jones, W.D. Bates, T.J. Meyer, J. Phys. Chem. 98 (1994) 10504.

[61] A.C. Benniston, A. Harriman, P.Y. Li, P.V. Patel, C.A. Sams, J. Org. Chem. 71 (2006) 3481.

[62] I. Llarena, A.C. Benniston, G. Izzet, D.B. Rewinska, R.W. Harrington, W. Clegg, Tetrahedron Lett. 47 (2006) 9135.

[63] A. El-ghayoury, A. Harriman, R. Ziessel, J. Phys. Chem. A 104 (2000) 7906.

[64] A. El-ghayoury, A. Harriman, A. Khatyr, R. Ziessel, J. Phys. Chem. A 104 (2000) 1512.

[65] A.C. Benniston, A. Harriman, D.B. Rewinska, S.Yang, Y.-G. Zhi, Chem. Eur. J., in press.

[66] A.C. Benniston, S. Mitchell, S.A. Rostron, S.J. Yang, Tetrahedron Lett. 45 (2004) 7883.

[67] A.C. Benniston, A. Harriman, S. Mitchell, S.A. Rostron, C.A. Sams, S.J. Yang, in preparation.

[68] A.C. Benniston, P.R. Mackie, A. Harriman, Angew. Chem., Int. Ed. Engl. 37 (1998) 354.

[69] J.-P. Collin, A. Harriman, V. Heitz, F. Odobel, J.-P. Sauvage, J. Am. Chem. Soc. 116 (1994) 5679.

[70] L. Flamigni, F. Barigelletti, N. Armaroli, B. Ventura, J.-P. Collin, J.-P. Sauvage, J.A.G. Williams, Inorg. Chem. 38 (1999) 661.

[71] L. Flamigni, F. Barigelletti, N. Armaroli, B. Ventura, J.-P. Collin, J.-P. Sauvage, J.A.G. Williams, Chem. Eur. J. 4 (1998) 1744.

[72] L. Flamigni, N. Armaroli, F. Barigelletti, V. Balzani, J.-P. Collin, J.-O. Dalbavie, V. Heitz, J.-P. Sauvage, J. Phys. Chem. B 101 (1997) 5936.

[73] I.M. Dixon, J.-P. Collin, J. Porphyrins Phthalocyanines 5 (2001) 600.

[74] A. Harriman, M. Hissler, O. Trompette, R. Ziessel, J. Am. Chem. Soc. 121 (1999) 2516.

[75] A.C. Benniston, G.M. Chapman, A. Harriman, C.A. Sams, Inorg. Chim. Acta 359 (2006) 753.

[76] A.C. Benniston, A. Harriman, P.Y. Li, C.A. Sams, J. Am. Chem. Soc. 127 (2005) 2553.

[77] A.C. Benniston, A. Harriman, D.J. Lawrie, A. Mayeux, Phys. Chem. Chem. Phys. 6 (2004) 51.

[78] A. Harriman, A. Mayeux, A. De Nicola, R. Ziessel, Phys. Chem. Chem. Phys. 4 (2002) 2229.

[79] A. Harriman, G. Izzet, Phys. Chem. Chem. Phys. 9 (2007) 944.

[80] A.C. Benniston, A. Harriman, P.Y. Li, C.A. Sams, J. Phys. Chem. A 109 (2005) 2302.

[81] V. Grosshenny, A. Harriman, J.P. Gisselbrecht, R. Ziessel, J. Am. Chem. Soc. 118 (1996) 10315.

[82] P.S. Braterman, A. Harriman, G.A. Heath, L.J. Yellowlees, J. Chem. Soc. Dalton Trans. (1983) 1801.

[83] R.A. Malone, D.F. Kelley, J. Chem. Phys. 95 (1991) 8970.

[84] A. Yeh, C. Shank, J. McCusker, Science 289 (2000) 935.

[85] G.B. Shaw, C.L. Brown, J.M. Papanikolas, J. Phys. Chem. A 106 (2002) 1483.

[86] J.R. Schoonover, D.M. Dattelbaum, A. Malko, V.I. Klimov, T.J. Meyer, D.J. Styers-Barnett, E.Z. Gannon, J.C. Granger, W.S. Aldridge, J.M. Papanikolas, J. Phys. Chem. A 109 (2005) 2472.

[87] R. Lomoth, T. Haupl, O. Johansson, L. Hammarström, Chem. Eur. J. 8 (2002) 102.

[88] S. Wallin, J. Davidsson, J. Modin, L. Hammarström, J. Phys. Chem. A 109 (2005) 4697.

[89] A.C. Benniston, A. Harriman, C. Pariani, C.A. Sams, J. Phys. Chem. A, in press.